Control of Protein−Protein Interactions: Structure-Based Discovery of Low Molecular Weight Inhibitors of the Interactions between Pin1 WW Domain and Phosphopeptides

Caroline Smet,[†] Jean-Frédéric Duckert,[†] Jean-Michel Wieruszeski,[†] Isabelle Landrieu,[†] Luc Buée,[‡] Guy Lippens,[†] and Benoît Déprez*,[†]

CNRS-University of Lille 2 UMR 8525, Institut Pasteur de Lille, Molecular Drug Discovery, 3 rue du Professeur Laguesse, 59000 Lille, France, and Inserm U422, place de Verdun, 59000 Lille, France

Received January 6, 2005

Interactions involving phosphorylated Ser/Thr-Pro motifs in proteins play a key role in numerous regulatory processes in the cell. Here, we investigate potential ligands of the WW binding domain of Pin1 in order to inhibit protein−protein interactions between Pin1 and phosphopeptides. Our structure-based strategy implies the synthesis of analogues of the Ac-Thr(PO_3H_2)-Pro-NH_2 dipeptide and relies on high resolution NMR spectroscopy to accurately measure the affinity constants even in the high micromolar range.

Introduction

Protein−protein interactions have an important role in most biological processes. A number of small domains present in various proteins with different biological functions are recurrent in protein−protein interactions and stand as such in the core of the cellular protein network.[1] Interactions mediated by phosphorylated moieties on their targets are of particular interest, since crucial regulation processes involve a balance between phosphorylation and dephosphorylation pathways allowed by kinase and phosphatase activities.[2]

Pin1 is a peptidyl-prolyl *cis*/*trans* isomerase constituted by two domains, a catalytic prolyl *cis*/*trans* isomerase domain and a WW binding module.[3] Both share a specificity for phospho-Thr/Ser-Pro motifs. At the cellular level, Pin1 is shown to be an essential protein involved in cell cycle regulation, since Pin1 inhibition prevents entry into mitosis and cell division.[4,5] Overexpression of Pin1 in numerous human cancers indicates its implication in several oncogenic pathways.[6,7] Therefore, Pin1 is proposed as a therapeutic target for cancer treatment.[8] Pin1 also interacts with the neuronal microtubule-associated tau protein when the latter is phosphorylated at specific motifs, and thereby restores its ability to polymerize the tubulin into microtubules.[9]

Inhibition of Pin1 activity with small molecules targeting the enzymatic domain blocks cell proliferation in cancer cell lines. Juglone was the first of this category of irreversible ligands, and the synthesis and characterization of several derivatives has been described.[10,11] Recently, conformationally constrained isosteres of phosphoSer-*cis*/*trans*-Pro were described in inhibition of *cis*/*trans* catalytic activity of Pin1.[12] The WW domain of Pin1, however, is equally essential for its *in vivo* activity.[5,13] Moreover, in healthy tissue, phosphorylation of the WW Ser16 inhibits its binding role and inactivates the whole protein. In breast cancer cells, the WW domain is dephosphorylated, leading to the active form of the protein.[14]

Structural data on Pin1 or isolated WW domain in complexes with phosphopeptides indicate an extremely limited interface between both partners, centered on phosphoThr-Pro dipeptide and a poor contribution of other sequential residues surrounding the dipeptide.[15,16] At the molecular level, the WW domain has a flexible loop encompassing Ser16-Ser19 residues that binds the phosphate moiety on Ser or Thr residues and an aromatic clamp constituted by its Tyr23 and Trp34 side chains that binds the prolyl residue in the +1 position of the phosphoSer/Thr (Figure 1).[15,16] These two points of interaction are of particular interest and are shared by other binding modules that display either the phospho specificity, distinctly for phosphoTyr (SH2,[17] PTB[18]) and phosphoSer/Thr (14−3−3 and FHA[19]), or affinity for proline-rich sequences like SH3 and other classes of WW domains (WW type I, II/III).[20,21] The phosphate moiety brings in strong hydrogen bonds toward the guanidine side chain and backbone amide groups, and is as such a real challenge to the development of potent mimetics.[22] On the other hand, proline displays a unique pattern among the 20 natural amino acids because its side chain is comprised in a five membered ring allowing a critical role in protein structuration (formation of β-turn or PP II helix in proline-rich peptides) or in protein−protein interactions.[21] Although steric and stereoelectronic effects of aryl-, alkyl-, and heteroatom-substituted prolines have been used to study factors that affect prolyl peptide conformation and activity,[23] the impact of such modifications on the recognition of the side chain itself is receptor dependent. Some examples have been described in the case of protease inhibitors.[24,25]

The present study is an exploration of both functional groups in the context of the Pin1 WW domain, using NMR spectroscopy throughout to evaluate the individual compounds.

* To whom correspondence should be addressed. Phone: +33/(0) 320964024. Fax: +33/(0) 320964709. E-mail: bdeprez@pharma.univ-lille2.fr.
[†] CNRS-University of Lille 2 UMR 8525.
[‡] Inserm U422.

10.1021/jm0500119 CCC: $30.25
Published on Web 06/25/2005

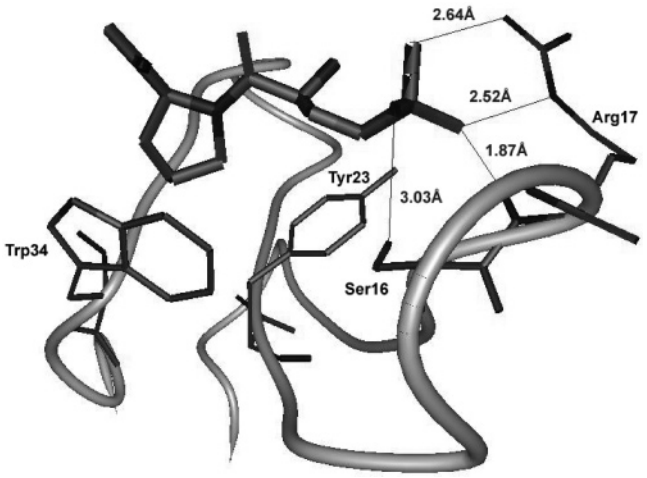

Figure 1. Structure of the dipeptide Ac-Thr(PO_3H_2)-Pro-NH_2 (**1a**) bound to the Pin1 WW domain. The WW domain is represented as ribbon and the substrate as thick sticks. Side chains of WW residues implicated in dipeptide binding are represented as thin sticks and annotated. Hydrogen bonds between phosphate and Ser16 hydroxyl group and Arg17 guanidinium function are indicated by lines and distances. The proline moiety is encompassed in an aromatic clamp constituted by side chains of Tyr23 and Trp34.

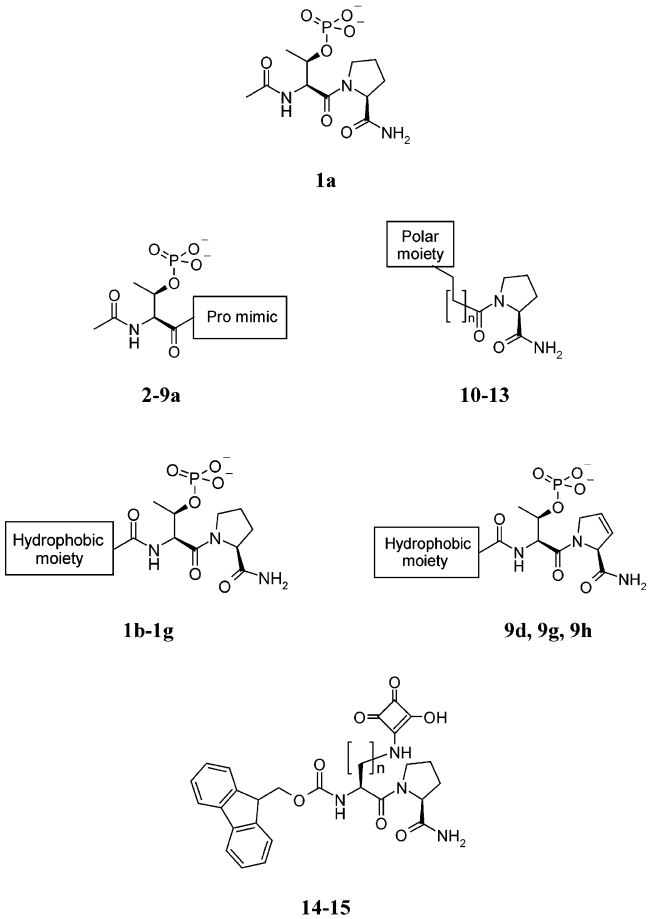

Figure 2. Structures of synthetic WW domain-binding analogues. Structure details of proline mimics and polar moieties are given in Table 1 and Table 2, respectively, and structures of hydrophobic moieties in Table 3.

The Ac-Thr(PO_3H_2)-Pro-NH_2 dipeptide **1a** (Figure 2) was assessed by NMR as the minimal requirement for binding to the Pin1 WW module exhibiting a relatively high dissociation constant of 150 μM and a similar mode of binding as larger peptidic substrates that derive from cell cycle-related proteins like RNA Pol II[15] and Cdc25 or the neuronal tau protein.[16,26] On the basis of the molecular structures of the WW domain and the ligand (**1a**), we investigate here potential ligands for the Pin1 WW binding domain, by sequentially considering compounds that contain proline or phosphate mimics, and further extending these compounds with additional hydrophobic moieties (Figure 2). High-resolution NMR proved a sensitive assay even for very weak ligands,[27,28] with cryogenic probe technology limiting appropriately the amount of protein and ligand.[29] Moreover, structural information could be obtained at every step through a simple mapping of chemical shift variations of the WW domain.

Results and Discussion

Synthesis. First, we have investigated separately the replacement of proline and the replacement of phosphothreonine in two series of molecules described in the template Figure 2: (i) proline mimics coupled to phosphothreonine through an amide bond in the compounds **2**−**9a** and (ii) polar moieties replacing phosphate supported by various backbone coupled to prolinamide in the compounds **10**−**13**. Then, introduction of hydrophobic moieties in compounds **1b**−**1g**, **9d**, **9g**, **9h**, **14**, and **15** was investigated in order to improve compound affinities for the WW module. Compounds **1**−**11** were synthesized by solid phase chemistry on polystyrene solid support functionalized by a rink amide linker (Scheme 1). The chemistry involved is very similar to solid phase peptide synthesis. Amine functions were protected by a Fmoc group and deprotected by suspending the resin in a 20% piperidine solution in DMF. Carboxylic acid activation was performed by a mixture of 1 equiv of HOBt/1 equiv of HBTU and 3 equiv of DIPEA in DMF. Cleavage of compounds from resin beads and deprotection of polar moiety (phosphate, carboxylate) were performed under high concentrations of TFA. Compounds **12**−**15** were synthesized by classical homogeneous phase synthesis by coupling amino acid derivatives of various chain lengths (β-alanine, ornithine, lysine) on prolinamide and functionalizing the amine group of these compounds with polar moieties (squarate, trifluoromethylsulfonyl) (Scheme 2).

Pin 1 WW Domain Expression, Purification, and NMR Characterization. The Pin1 WW binding module [Ala_2−Asn_{40}] was cloned in a pET28 plasmid fusioned to an N-terminal His_6 tag and overexpressed in *Escherichia coli* that allows uniform isotopic labeling of the protein for NMR studies. The protein was purified from the soluble cell lysate using two chromatography systems: chromatography based on nickel affinity and reverse phase high pressure liquid chromatography. The protein was obtained at a degree of purity superior to 95% (SDS−PAGE) and characterized by matrix-assisted laser desorption ionization time-of-flight (MALDI-TOF) mass spectrometry and high resolution NMR. After purification, the Pin1 WW domain spontaneously folded when dissolved in NMR buffer, and bound correctly to phosphorylated tau peptides as assessed by NMR or FRET experiments.[26] No detectable interaction was observed with nonphosphorylated peptides. Initially, the

Scheme 1. [a] General Scheme of Synthesis for Compounds **1**−**11**

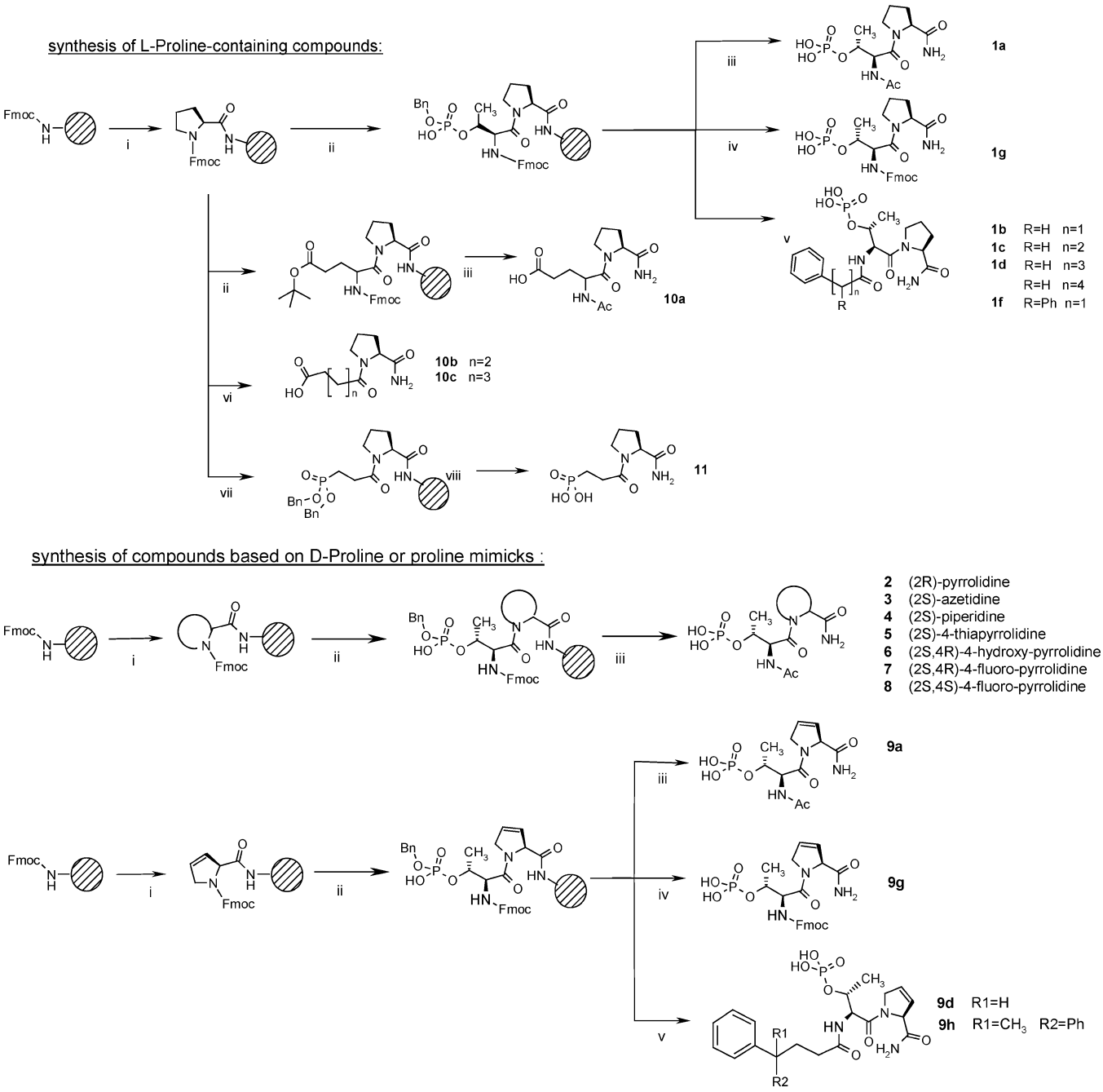

[a] Reagents and conditions: (i) (a) piperidine 20%, DMF, room temperature, 25 min; (b) *N*-Fmoc-(L)-Pro-OH or mimetics, HOBt, HBTU, 3 equiv of DIPEA, DMF, room temperature, 1 h; (ii) (a) piperidine 20%, DMF, room temperature, 25 min; (b) *N*-Fmoc-(L)-Thr(PO(OBn)OH)-OH or *N*-Fmoc-(L)-Glu(tBu)-OH, HOBt, HBTU, 3 equiv of DIPEA, DMF, room temperature, 1 h; (iii) (a) piperidine 20%, DMF, room temperature, 25 min; (b) Ac_2O, 3 equiv of DIPEA, DMF, room temperature, 30 min; (c) TFA 95%, TIS 2.5%, water 2.5%, room temperature, 5 h; (iv) TFA 95%, TIS 2.5%, water 2.5%, room temperature, 5 h; (v) (a) piperidine 20%, DMF, room temperature, 25 min; (b) carboxylic acid precursor, HOBt, HBTU, 3 equiv of DIPEA, DMF, room temperature, 1 h; (c) TFA 95%, TIS 2.5%, water 2.5%, room temperature, 5 h; (vi) (a) piperidine 20%, DMF, room temperature, 25 min; (b) glutaric anhydride or succinic anhydride, 3 equiv of DIPEA, DMF, room temperature, 1 h; (c) TFA 95%, TIS 2.5%, water 2.5%, room temperature, 2 h; (vii) (a) piperidine 20%, DMF, room temperature, 25 min; (b) 3-(dibenzyloxyphosphoryl)-propionic acid, HOBt, HBTU, 2 equiv of DIPEA, DMF, room temperature, 6 h; (viii) (a) TFA 95%, TIS 2.5%, water 2.5%, room temperature, 5 h; (b) H_2 at atmospheric pressure, Pd/C 10%, MeOH, room temperature, 48 h.

protein was assigned using conventional tridimensional NMR experiments (HNCA, HNCO, and HN(CO)CA) on a 500 μM $^{15}N/^{13}C$-labeled protein sample on a 600 MHz spectrometer (Bruker, Karlsruhe, Germany)).

Discovery of Novel Reversible Ligands for the Pin1 WW Binding Module. In an initial phase, we screened compounds by rapid 1D NMR experiments at a 20-fold excess of ligand to WW domain. The WW domain at 20 μM was ^{15}N-labeled, allowing the efficient filtering of the ligand resonances. The signal of the HNϵ of the Trp34 (at 10.2 ppm) was used as a sensitive probe to detect perturbations of the Trp side chain chemical environment upon binding of the proline ring. When interaction was detected, we performed an additional titration study with a 50 μM ^{15}N-labeled WW sample and increasing amounts of ligands (from 0.5 to 20 equiv).

Scheme 2. [a] General Scheme of Synthesis for Compounds **12**−**15**

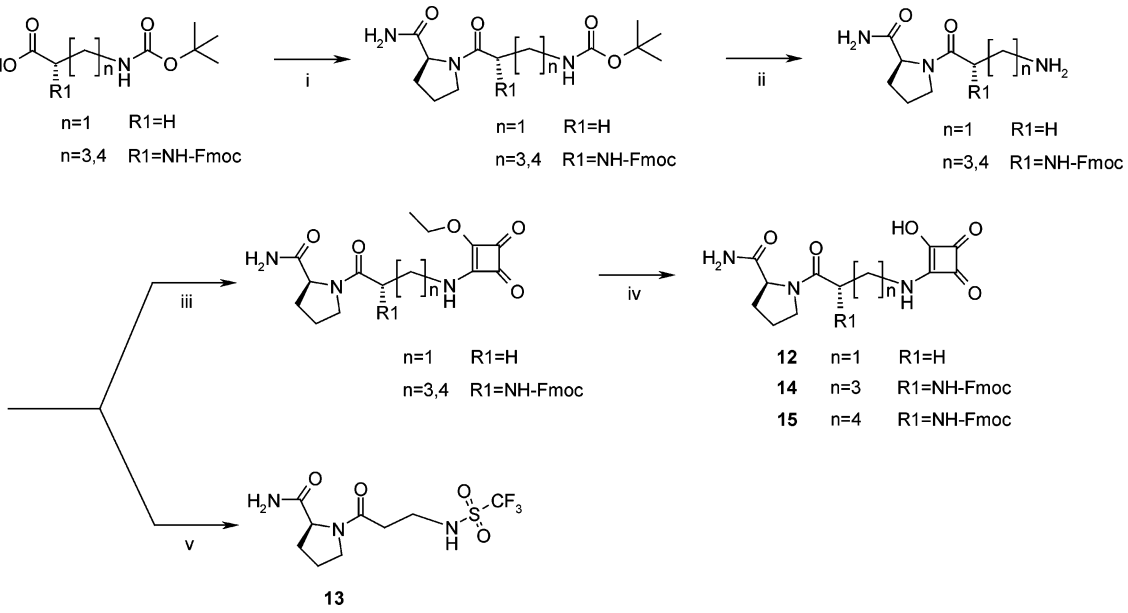

[a] Reagents and conditions: (i) (a) DCC/DCM; (b) prolinamide/DCM, 0 °C, 2 h; (ii) HCl/dioxane, 0 °C then room temperature, 3 h; (iii) (a) NEt_3/EtOH; (b) diethylsquarate/EtOH, room temperature, 12 h; (iv) HCl/DCM room temperature, 24 h; (v) (a) NEt_3/DCM; (b) trifluorosulfonyl chloride/DCM, room temperature, 48 h.

Gradual chemical shift perturbations with increasing ligand concentrations were used to derive the dissociation constant (Figure 3).

The aromatic clamp was found to accept Pro mimics with structural variations of the pyrrolidine ring. Despite the relatively low affinities, NMR titrations yielded reliable SAR results for analogues of Ac-Thr(PO_3H_2)-Pro-NH_2 (**2**−**9a**). Compounds where the pyrrolidine ring is replaced by an azetidine or a piperidine bind the WW domain without significant changes of affinity. The same observation is made for the epimer at the Cα of proline. Substitutions have contradictory effects on binding since the replacement of proline by 4-*trans*-hydroxyproline, 4-*cis*-fluoroproline, or thiazolidine-4-carboxylic acid isostere decreases dramatically the affinity for the WW domain. However replacement of proline with a 4-*trans*-fluoroproline improves significantly the binding as well as the introduction of an unsaturation at position 3−4 of the pyrrolidine ring (Table 1). Contrary to the proline mimics, polar groups used to replace the phosphate moiety all exhibited dissociation constants as low as 2 mM, pointing out an extreme specificity of the flexible loop for phosphate binding (Table 2).

Faced with restricted possibilities for structural modifications around the two major points of interaction of dipeptide **1a** with the WW domain, we have examined further WW hydrophobic patches in the near proximity of the main binding site in order to gain in affinity. A potential hydrophobic surface constituted by Phe25 and Ala31 was targeted with a phenyl ring anchored to the Thr(PO_3H_2)-Pro dipeptide via aliphatic chains of various lengths in compounds **1b**−**1f** and with the Fmoc group in compound **1g**. A significant increase of binding affinity was observed for these compounds with a maximum for the 4-phenylbutyric acid precursor and for the Fmoc group that confirms the agreement with the 4-carbon-length chain (Table 3). Nevertheless, interactions with the phosphate binding loop and the prolyl ring binding pocket remain essential and appear as a minimal requirement for ligands to adapt the domain since the replacement of phosphothreonine by a glutamic acid in dipeptides carrying the same hydrophobic moieties did not significantly bind the WW domain (data not shown).

Consistency of Binding Mode in the Series. Chemical shift interaction mapping was performed for each compound of significantly improved affinity, to verify the consistency of the binding mode. Very similar modes of binding were observed for the various proline mimics in comparison with the dipeptide **1a**. The 3,4-dehydroproline moiety induces larger chemical shift perturbations for both phosphate and proline binding sites, and especially a stronger effect on the Y23 amide peak (Figure 4A), together with a significant line broadening concerning most of the interacting residues. The binding site of the hydrophobic moiety that replaces the acetyl group in the phospho-Thr-Pro dipeptide is given by the chemical shift mapping of compounds **1b**−**1g**. Larger Ala31 amide shifts (Figure 4B) and a dependence of the Ala31 variations with the chain length carrying a phenyl group (**1b**−**1e**) that is not shared by Trp34 or Arg17 verify our initial structural hypothesis. It cannot be ruled out that observed chemical shift variations could also be due to conformational changes of the domain upon ligand binding. However, since little variations are observed at remote amino acids from the binding pocket, we reasonably make the assumption that, in the series, the conformation of the WW domain in its ligand bound state is not strongly affected.

Combining the data on chain length and nature of the aromatic group with the previously determined optimal proline mimics provides a further perspective for improving the affinity. The combination of the three essential motifs was further investigated in compounds **9d**, **9g**, **9h** on the basis of the 3,4-dehydroproline analogue (Figure 2). In the proline series (**1b**−**1g**), the

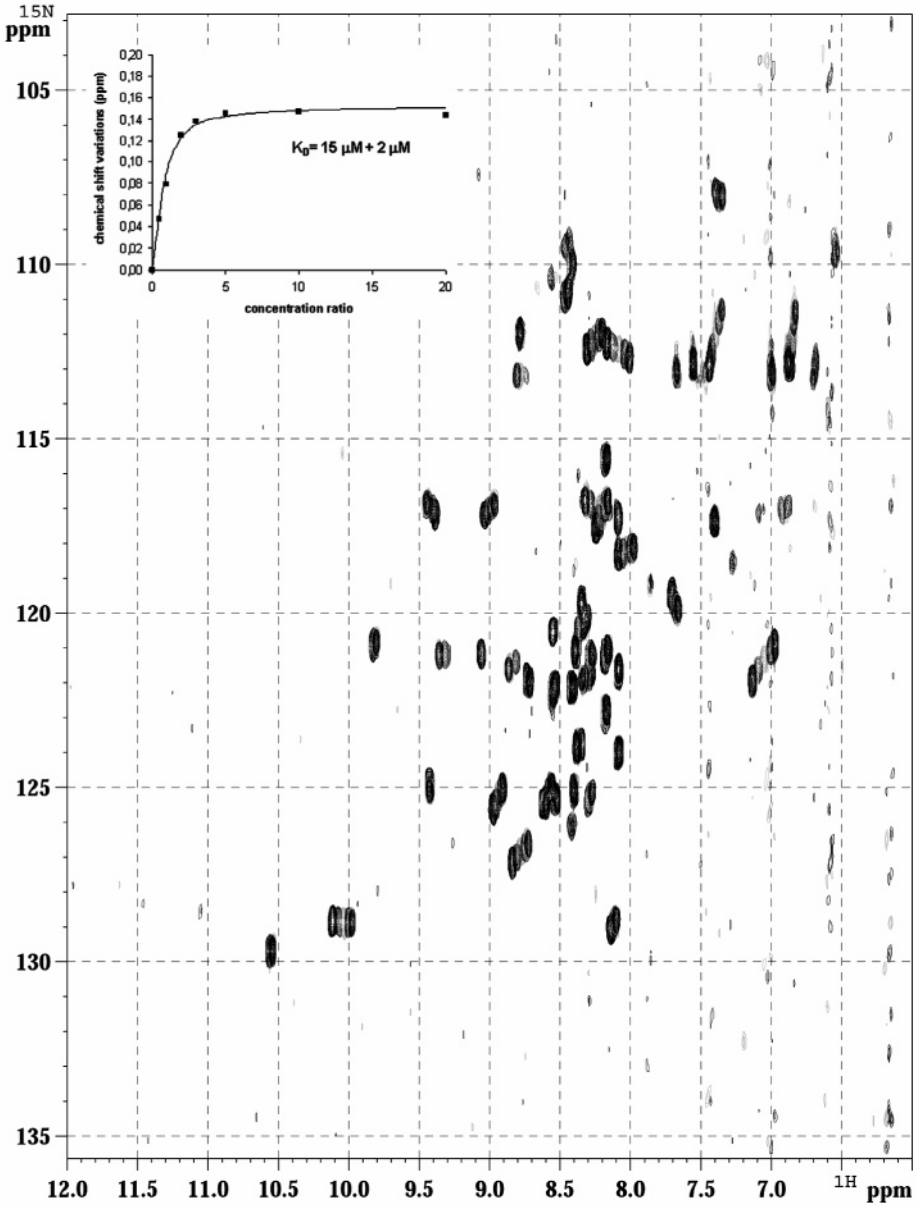

Figure 3. NMR titration of the ^{15}N-labeled WW domain with the ligand **1g**. Overlaid ^{1}H−^{15}N HSQC spectra acquired on a 50 μM WW domain ^{15}N-labeled sample with increasing amounts of compound **1g**. In the left top corner, a titration curve plotting the chemical shift variations against the concentration ratio **1g**:WW.

replacement of the acetyl group by ω-arylalkanoyl chains or a Fmoc group increased affinity as expected. Surprisingly, except for 4,4-bis(4-hydroxyphenyl)pentanoyl (**9h**), most of the hydrophobic moieties induce a decrease of affinity (Table 3) in the dehydroproline series, suggesting different structural constraints in the free ligand of both series.

Revisiting Phosphate Mimics on Improved Ligands. The ligands containing an additional point of interaction with the WW domain through the hydrophobic moiety display affinities in the low micromolar range. This level of affinity allows us to revisit possible phosphate isosteres. Squaramide is singly charged at physiological pH and thanks to delocalization of this charge can accept strong hydrogen bonds at each of its oxygen atoms. Compounds carrying this group instead of the phosphate were synthesized, and their binding was studied by NMR. In the Fmoc series, compounds **14** and **15** displayed measurable affinities (respectively 910 and 540 μM), thereby providing new entry points in series where the phosphate moiety could be replaced by an isosteric group. This provides new perspectives for improvement of metabolic stability and cell membrane permeation.

Perspectives in Disrupting Protein−Protein Interactions and Compound Activity in a Cell-Based Assay. To confirm that our small ligands can actually disrupt interactions between the WW binding module and its proline-containing substrates, we have conducted competition experiments using fluorescence energy transfer. Our ligands were tested for their ability to displace a tetradecapeptide centered on the Thr^{212}(PO_3H_2)-Pro^{213} of Tau protein[26] from the WW domain. In this setup, our best ligands were shown to displace the peptide with K_i consistent with their K_d (data not shown).

We have tested some of our lead compounds in a cellular model of SY5Y neuroblastoma cells with induc-

Table 1. Structures of Proline Mimics and Dissociation Constants of Resulting Ligands (**2**−**9a**)

compound	Pro mimic structures	K_D (μM)
2	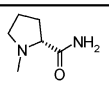	100
3	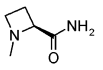	160
4	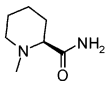	140
5	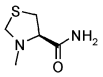	400
6	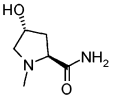	800
7	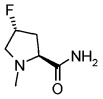	36
8	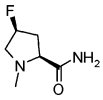	420
9a	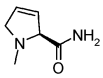	18

ible overexpression of Pin1. This cellular assay is based on the monitoring of cyclin D1 level as described.[30] In that model, juglone is used as a reference compound for the inhibition of Pin1 function and induces a marked diminution of the intracellular concentration of cyclin D1. Our results with WW ligands are at this moment very preliminary. Compound **1g** has produced the same effect as juglone at similar concentrations and poses the intriguing question whether it acts directly on Pin1 or also on other target(s). Further assays will be performed in the future to identify the cellular target(s) of our compounds.

Conclusion

Our NMR-based strategy has led to the conception, synthesis, and testing of new ligands for the Pin1 WW domain. Whereas the proline in the initial phospho-Thr-Pro dipeptide could be successfully replaced by a 3,4-dehydro- or 4-*trans*-fluoroproline, the specificity for the phosphate moiety proved more challenging. On the basis of the structure of the WW domain, we extended these ligands with an N-terminal aromatic group, resulting in a new series of ligands with low micromolar affinity. NMR proved crucial throughout this development, as a technique to bridge the gap between very low affinity hit compounds and conventional tools to measure affinity of small molecules to protein, such as fluorescence polarization or energy transfer. It allowed initial screening, and generated reliable SAR at low levels of affinity, as well as structural information on the binding mode of our ligands. The exact mode of action of our ligands is currently being studied.

Table 2. Structures of Polar Moieties and Dissociation Constants of Resulting Ligands (**10**−**13**)

compound	Polar moiety structures	K_D (μM)
10a	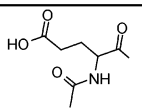	> 2000
10b	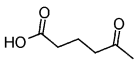	> 2000
10c	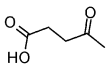	> 2000
11	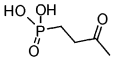	> 2000
12	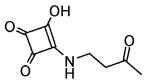	> 2000
13	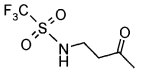	> 2000

Experimental Section

Protected natural amino acid, coupling reagents (HOBt and HBTU), and resin (polystyrene cross-linked with 2% divinylbenzene carrying a rink amide MBHA linker) were purchased from Novabiochem. Purity was checked by HPLC and LC−MS systems. LC−MS data were recorded on a Varian 1200 MS system using a TSKgel OSH supelco column. Water (A) and acetonitrile (B) containing 0.1% and 0.12% formic acid, respectively, were used as eluents. After sample injection, the column is equilibrated in solution A for 2 min and a 0−100% B 7.30 min-gradient is performed at a flow rate of 1 mL/min to elute compounds that are detected at 215 and 254 nm. HPLC data are collected on a C18 nucleosil column equilibrated in an aqueous solution containing 0.05% TFA (solution A). The eluent (solution B) contains 80% acetonitrile and 0.05% TFA. After sample injection, the column is washed with solution A for 5 min and then a 0−100% B 30 min gradient is performed at a flow rate of 1 mL/min. Compounds are detected at 215 nm. Characterization of compounds dissolved in DMSO-d_6 was also done with ^{1}H and ^{13}C NMR spectra recorded at 300 K on a 300 MHz Bruker spectrometer equipped with a BBI probehead.

General Procedure (A) for Synthesis of Compounds 1 to 11. Removal of Fmoc Protecting Group. Cleavage of the Fmoc group was performed with 20% piperidine in DMF (v/v). The resin beads were mixed with the previous solution (3 mL for 300 mg resin), and the reaction was performed at room temperature for 25 min. The solution was removed by filtration under vacuum, and the resin beads were extensively washed with DMF.

Coupling of Amino Acids. A mixture of 3 equiv of Fmoc protected amino acid, 3 equiv of HOBt, 3 equiv of HBTU dissolved in DMF, and 9 equiv of DIPEA were added to the resin beads. The reaction was performed at room temperature for 1 h. The solution was removed by filtration under vacuum, and the resin beads were extensively washed with DMF.

Table 3. Structures of Hydrophobic Moieties and Dissociation Constants of Resulting Ligands Based on Proline (**1b**−**1g**) or on 3,4-Dehydroproline (**9d**, **9g**, **9h**) Derivatives

compound	**1b**	**1c**	**1d**	**9d**	**1e**	**1f**	**1g**	**9g**	**9h**
Hydrophobic moiety structures			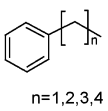 n=1,2,3,4			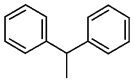	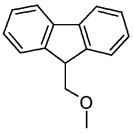		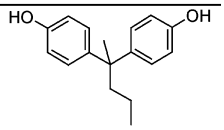
n =	1	2	3	3	4				
K_D (μM)	35	32	30	28	48	38	15	66	5

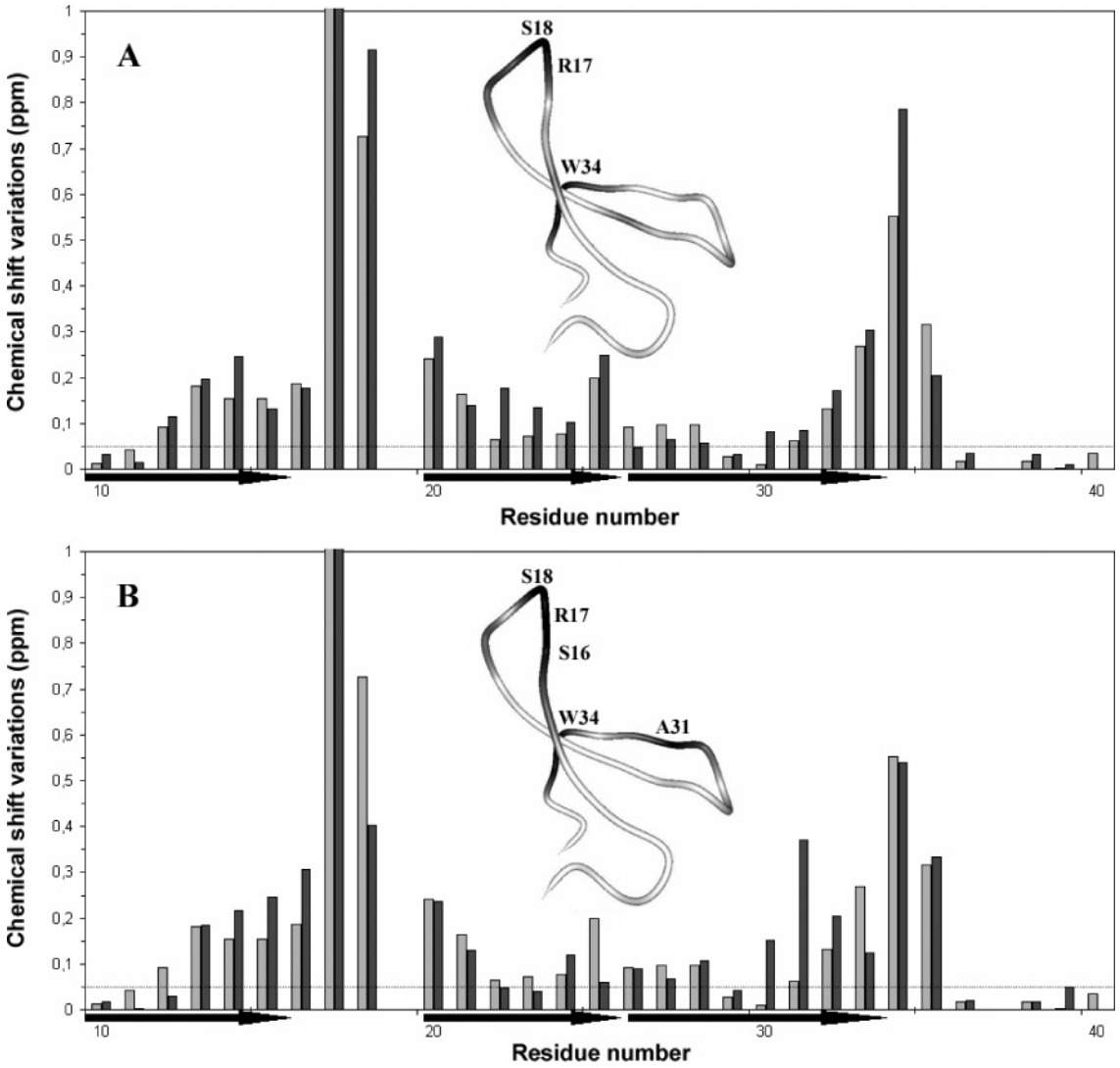

Figure 4. NMR chemical shift mapping of the ^{15}N-labeled WW domain. Comparison of the mapping of the WW domain in the presence of 20 equiv of compound **1a** in light gray and (A) compound **9a** or (B) compound **1g** in dark gray. Arrows along the *x*-axis indicate *β*-sheet structural elements. In the structure, the ribbon is darkened as a function of chemical shift variations of compound **9a** (A) and compound **1g** (B). Amino acids that display a variation superior to 0.3 ppm are labeled.

Amine Acetylation. Five equivalents of acetic anhydride was dissolved in DMF, and 10 equiv of DIPEA was added. The solution was mixed with the resin beads, and the mixture was agitated at room temperature for 30 min. The solution was removed by filtration under vacuum, and the resin beads were extensively washed with DMF.

Coupling of Hydrophobic Moieties. A mixture containing the carboxylic acid derivative (5 equiv), HOBt (5 equiv), and HBTU (5 equiv) and DIPEA (10 equiv) in DMF was added to the resin beads, and the coupling reaction was performed at room temperature for 1 h. The solution was removed by filtration under vacuum, and the resin beads were extensively washed with DMF.

TFA Cleavage of Resin-Bound Compounds and Benzyl Protecting Group. Resin beads were extensively washed with DMF, DCM, and 10% TFA in DCM and then mixed with a TFA solution containing 2.5% triisopropylsilane (v/v) and 2.5% water (v/v) (5 mL for 300 mg of resin). The heterogeneous mixture was placed under agitation for 5 h at room temperature. The solution was then filtered under vacuum, and the

resin was washed twice with TFA (2.5 mL each). The combined filtrates were collected in 200 mL of a cold mixture of ether/pentane (v/v). A white precipitate was formed, and the precipitation was achieved at −20 °C overnight. The precipitate was isolated by filtration, washed with ether, and then dissolved in water and lyophilized.

General Procedure (B) for Synthesis of Compounds 12 to 15. Coupling of Carboxylic Acid Derivatives on Prolinamide. Three equivalents of carboxylic acid derivative (*N*-α-Fmoc-ornithine/lysine(Boc) or *N*-Boc-*β*-alanine) was dissolved in DCM (15.8 mmol in 8 mL) and added to a solution of 1.5 equiv of DCC in DCM at 0 °C (7.9 mmol in 2 mL). The precipitate was filtered off, and the filtrate was added to a solution of 1 equiv of prolinamide in DCM (5.25 mmol in 3 mL). The reaction mixture was stirred for 2 h at 0 °C. The crude mixture was evaporated and dissolved in DCM. The precipitate was removed by filtration, and the organic layer was washed twice with a saturated $NaHCO_3$ aqueous solution and then dried over $MgSO_4$ and evaporated. Products were isolated by purification on silica column in DCM/EtOH 95/5.

Removal of Boc Protecting Group. One equivalent of the Boc protected compound was dissolved in DCM (1.37 mmol in 14 mL), and the mixture was cooled in an ice bath. A solution of 4 N HCl in dioxane was added dropwise to the previous solution at 0 °C. The mixture was stirred at room temperature for 3 h, and then the crude mixture was evaporated. The deprotected product is obtained in quantitative yield.

Coupling of Diethylsquarate. A solution of 1.2 equiv of diethylsquarate in ethanol (1.64 mmol in 5 mL) was prepared. One equivalent of *β*-alanine or *N*-α-Fmoc-ornithine/lysine coupled to prolinamide was dissolved in ethanol (1.37 mmol in 8 mL), and 1.5 equiv of triethylamine was added. The mixture was added dropwise to the diethylsquarate solution, and the reaction was performed at room temperature for 12 h. The crude mixture was evaporated, dissolved in DCM, and purified on a silica column in DCM/MeOH 9/1.

Removal of Ethyl Protecting Group. The ethylsquarate derivative was dissolved in THF (1.084 mmol in 6 mL) and stirred with a solution of 4 N HCl in THF (12 mmol in 3 mL) at room temperature for 20 h. The crude mixture was evaporated. The powder was dissolved in DCM and extracted four times with a 0.3 N solution of ammonium carbonate. The aqueous solution was lyophilized.

Coupling of Trifluoromethylsulfochloride. Triethylamine (1.2 equiv, 1.044 mmol, 146 μL) was added to 1 equiv of *β*-alanine coupled to prolinamide dissolved in DCM. Trifluorosulfonyl chloride (1.2 equiv, 1.044 mmol, 110 μL) was dissolved in 10 mL of DCM and added to the previous solution dropwise. The mixture was stirred at room temperature for 48 h. The crude mixture was evaporated, dissolved in DCM, and purified on a silica column in DCM/EtOH 8/2.

Peptide Synthesis (for IC_{50} Determination). The peptide sequence was isolated from the Tau protein around the Thr212-Pro213 epitope as described.[26] The phosphorylated peptide was obtained by solid phase synthesis with introduction of selectively phosphorylated threonine using appropriate building block (Novabiochem). The dansyl fluorescent probe (Sigma) was introduced selectively at the N-terminus by reaction of dansyl chloride (5 equiv) and DIPEA (10 equiv) in DMF and followed by a TFA cleavage. Peptide was isolated by precipitation of the TFA solution in 200 mL of a cold mixture of ether/heptane (v/v) and centrifugation. The peptide was dissolved in water and purified by RP-HPLC on a C18 nucleosil column equilibrated in a 0.05% TFA aqueous solution (solution A). Separation of peptides in the crude mixture was carried out at 50 °C at a flow rate of 2 mL/min using an acetonitrile linear 60 min gradient from 0 to 50% solution B (80% acetonitrile:20% water−0.05% TFA). Homogeneous fractions as checked by RP-HPLC on a C18 nucleosil column (0 to 100% B linear 30 min gradient) and MALDI-TOF MS were pooled and lyophilized.

Protein Expression and Purification. The WW domain was produced in *E. coli* BL21(DE3) strain, carrying the pET28a plasmid under control of T7 promoter with a sequence encoding a N-terminus His_6 tag. Cells were grown at 37 °C in a LB medium containing kanamycin (20 mg/L) until O.D. at 600 nm reached about 0.6, allowing a rapid growth to high cell density. Then cells were harvested by centrifugation. The pellet was resuspended in a M9 medium containing 4 g/L glucose, 1 g/L $^{15}NH_4Cl$, 1 mM $MgSO_4$, 20 mg/L kanamycin, and MEM vitamin cocktail (Sigma) and incubated at 37 °C for 1 h. Induction was performed with 0.5 mM IPTG (at final concentration) at 31 °C for 3 h. Cells were harvested by centrifugation, and the pellet was resuspended in 50 mM Na_2HPO_4/NaH_2PO_4 pH 8.0, 300 mM NaCl buffer (buffer A) containing 10 mM imidazole, 1 mM DTT, 0.1% NP40 and complemented with a protease inhibitor cocktail (Roche). The soluble lysate was obtained by sonication and centrifugation. The soluble extract was charged on a nickel-nitrilotriacetic affinity column (Chelating Sepharose Fast Flow, Amersham). Unbound proteins were washed with 20 mM imidazole in buffer A, and the WW domain was eluted with 250 mM imidazole in buffer A (pH 7.8). The protein was then purified by RP-HPLC on a Source 15RPC column (Amersham) equilibrated in a 0.05% TFA aqueous solution (solution A). Separation of proteins was carried out at room temperature at a flow rate of 1 mL/min using an acetonitrile linear 20 min gradient from 0 to 60% solution B (85% acetonitrile:15% water−0.05% TFA). Homogeneous fractions as checked by SDS−polyacrylamide gel electrophoresis were pooled and lyophilized.

NMR Screening. NMR experiments were performed on a Bruker DMX 600 MHz spectrometer at 293 K equipped with a cryogenic probehead. ^{15}N-labeled WW was dissolved in 25 mM deuterated Tris-HCl (pH = 6.8) aqueous buffer containing 50 mM NaCl, 5 mM DTT, and 2.5 mM EDTA and 10% D_2O. The spectra were referenced to the signal of sodium 3-trimethylsilyl-d(3,3′,2,2′)-propionate (TSPA-d_4). A solution of ^{15}N-labeled WW at 200 μM (60 μL) was added to a 2 mM solution of ligand (120 μL) to reach final concentrations (in 600 μL) of 20 μM WW and 400 μM ligand in the NMR sample buffer.

NMR Dissociation Constant Calculation. Lyophilized aliquots of ligand were prepared from a concentrated solution (2 mM) to get a concentration range of 0.025, 0.05, 0.1, 0.15, 0.25, 0.5, and 1 mM (at final concentration in 600 μL of protein solution). A solution of 50 μM ^{15}N-labeled WW was added to lyophilized aliquots of ligands. Quantification of chemical shift perturbations was calculated according to eq 1.

$$\Delta\delta(\text{ppm}) = \sqrt{\Delta\delta(^1\text{H})^2 + 0.2\Delta\delta(^{15}\text{N})^2} \quad (1)$$

$\Delta\delta(^1H)$ and $\Delta\delta(^{15}N)$ are the chemical shift variations of amide proton (H_N) and amide nitrogen (N_H), respectively, of WW domain residues the upon ligand addition.

Dissociation constants were calculated by fitting on a graphical representation the theoretical curve obtained from eq 2 with experimental points.

$$\Delta\delta(\text{ppm}) = 0.5\Delta\delta_{\max}\left(1 + X + \frac{K_D}{[\text{protein}]_0} - \sqrt{\left(1 + X + \frac{K_D}{[\text{protein}]_0}\right)^2 - 4X}\right) \quad (2)$$

X is the molar ratio of ligand on protein, $[\text{protein}]_0$ the initial concentration of protein, and $\Delta\delta$ the chemical shift variation calculated using eq 1. $\Delta\delta_{max}$ was set at the $\Delta\delta$ value at the protein saturation level.

FRET Competition Experiments for IC_{50} Determination. FRET experiments were achieved on a PTI fluorescence spectrometer by exciting tryptophan residues of WW domain at 295 nm. As for NMR titrations, a 20 μM solution of WW in protonated Tris 50mM pH 6.8 buffer containing 50 mM NaCl and 5 mM DTT/EDTA and various concentrations of dansylated peptide were added on lyophilized aliquots of ligand. The dissociation constant of the WW−peptide complex was evalu-

ated to 100 μM according to eq 2 by replacing $\Delta\delta$ with ΔI^{334}, the intensity variation of the fluorescence emission signal measured at 334 nm.[26] IC_{50} determination was calculated as described for dissociation constants determined by NMR with eq 2 by replacing $\Delta\delta$ with the inhibition percentage given by eq 3 and K_D by IC_{50}.

$$\% \text{ inhibition} = \frac{I^{334} - I_0^{334}}{I_0^{334} - I_{100}^{334}} \quad (3)$$

I^{334} is the fluorescence intensity at 334 nm upon ligand addition, I_0^{334}, the fluorescence intensity without inhibition, and I_{100}^{334}, the fluorescence intensity at maximal inhibition.

Acknowledgment. The authors thank the Institute for the Study Of Aging (ISOA, the United States) for financial support. We thank Professor André Tartar for fruitful discussions, Gérard Montagne, Hervé Drobecq, and Eric Diesis for their technical contribution to this work and Dr. Dragos Horvath for molecular modeling. The 600 MHz facility used in this study was funded by the Région Nord-Pas de Calais (France), the CNRS, and the Institut Pasteur de Lille.

Appendix

Abbreviations. MBHA, 4-methylbenzhydrylamine; HOBt, 1-hydroxybenzotriazole; HBTU, 2-(1*H*-benzotriazol-1-yl)-1,1,3,3-tetramethyluronium hexafluorophosphate; Fmoc, 9-fluorenylmethoxy-carbonyl; K_D, dissociation constant; IC_{50}, inhibition constant at 50%; Boc, *tert*-butoxycarbonyl; Bzl, benzyl; DCM, dichloromethane; DMF, dimethylformamide; EtOH, ethanol; DMSO, dimethyl sulfoxide; DIPEA, diisopropylethylamine; TFA, trifluoroacetic acid; DTT, dithiothreitol; EDTA, ethylenediaminetetraacetic acid; HSQC, heteronuclear simple quantum correlation; Tris, 2-amino-2-hydroxymethyl-1,3-propanediol; BBI, inverse broad band (probe); MALDI-TOF, matrix assisted laser desorption ionization time-of-flight; RP-HPLC, reverse phase high pressure liquid chromatography; SDS−PAGE, sodium dodecyl sulfate−polyacrylamide gel electrophoresis.

Supporting Information Available: Synthetic procedures and spectral characterization of compounds **1a** to **15**. This material is available free of charge via the Internet at http://pubs.acs.org.

References

(1) Pawson, T.; Raina, M.; Nash, P. Interaction domains: from simple binding events to complex cellular behavior. *FEBS Lett.* **2002**, *513*, 2−10.
(2) Yaffe, M. B.; Smerdon, S. J. The Use of in Vitro Peptide-Library Screens in the Analysis of Phosphoserine/Threonine-Binding Domain Structure and Function. *Annu. Rev. Biophys. Biomol. Struct.* **2004**, *33*, 225−244.
(3) Ranganathan, R.; Lu, K. P.; Hunter, T.; Noel, J. P. Structural and functional analysis of the mitotic rotamase Pin1 suggests substrate recognition is phosphorylation dependent. *Cell* **1997**, *89*, 875−886.
(4) Lu, K. P.; Hanes, S. D.; Hunter, T. A human peptidyl-prolyl isomerase essential for regulation of mitosis. *Nature* **1996**, *380*, 544−547.
(5) Winkler, K. E.; Swenson, K. I.; Kornbluth, S.; Means, A. R. Requirement of the prolyl isomerase Pin1 for the replication checkpoint. *Science* **2000**, *287*, 1644−1647.
(6) Wulf, G.; Ryo, A.; Liou, Y. C.; Lu, K. P. The prolyl isomerase Pin1 in breast development and cancer. *Breast Cancer Res.* **2003**, *5*, 76−82.
(7) Wulf, G. M.; Ryo, A.; Wulf, G. G.; Lee, S. W.; Niu, T.; et al. Pin1 is overexpressed in breast cancer and cooperates with Ras signaling in increasing the transcriptional activity of c-Jun towards cyclin D1. *Embo J.* **2001**, *20*, 3459−3472.
(8) Lu, K. P. Prolyl isomerase Pin1 as a molecular target for cancer diagnostics and therapeutics. *Cancer Cell* **2003**, *4*, 175−180.
(9) Lu, P. J.; Wulf, G.; Zhou, X. Z.; Davies, P.; Lu, K. P. The prolyl isomerase Pin1 restores the function of Alzheimer-associated phosphorylated tau protein. *Nature* **1999**, *399*, 784−788.
(10) Uchida, T.; Takamiya, M.; Takahashi, M.; Miyashita, H.; Ikeda, H. et al. Pin1 and Par14 peptidyl prolyl isomerase inhibitors block cell proliferation. *Chem. Biol.* **2003**, *10*, 15−24.
(11) Hennig, L.; Christner, C.; Kipping, M.; Schelbert, B.; Rucknagel, K. P.; et al. Selective inactivation of parvulin-like peptidyl-prolyl cis/trans isomerases by juglone. *Biochemistry* **1998**, *37*, 5953−5960.
(12) Wang, X. J.; Xu, B.; Mullins, A. B.; Neiler, F. K.; Etzkorn, F. A. Conformationally locked isostere of phosphoSer-cis-Pro inhibits Pin1 23-fold better than phosphoSer-trans-Pro isostere. *J. Am. Chem. Soc.* **2004**, *126*, 15533−15542.
(13) Lu, P. J.; Zhou, X. Z.; Shen, M.; Lu, K. P. Function of WW domains as phosphoserine- or phosphothreonine-binding modules. *Science* **1999**, *283*, 1325−1328.
(14) Lu, P. J.; Zhou, X. Z.; Liou, Y. C.; Noel, J. P.; Lu, K. P. Critical role of WW domain phosphorylation in regulating phosphoserine binding activity and Pin1 function. *J. Biol. Chem.* **2002**, *277*, 2381−2384.
(15) Verdecia, M. A.; Bowman, M. E.; Lu, K. P.; Hunter, T.; Noel, J. P. Structural basis for phosphoserine-proline recognition by group IV WW domains. *Nat. Struct. Biol.* **2000**, *7*, 639−643.
(16) Wintjens, R.; Wieruszeski, J. M.; Drobecq, H.; Rousselot-Pailley, P.; Buee, L. et al. 1H NMR study on the binding of Pin1 Trp-Trp domain with phosphothreonine peptides. *J. Biol. Chem.* **2001**, *276*, 25150−25156.
(17) Songyang, Z.; Shoelson, S. E.; Chaudhuri, M.; Gish, G.; Pawson, T. et al. SH2 domains recognize specific phosphopeptide sequences. *Cell* **1993**, *72*, 767−778.
(18) Yan, K. S.; Kuti, M.; Zhou, M.-M. PTB or not PTB- that is the question. *FEBS Lett.* **2002**, *73*, 67−70.
(19) Yaffe, M. B.; Elia, A. E. H. Phosphoserine/threonine-binding domains. *Curr.Opin. Cell Biol.* **2001**, *13*, 131−138.
(20) Macias, M. J.; Wiesner, S.; Sudol, M. WW and SH3 domains, two different scaffolds to recognize proline-rich ligands. *FEBS Lett.* **2002**, *513*, 30−37.
(21) Kay, B. K.; Williamson, M. P.; Sudol, M. The importance of being proline: the interaction of proline-rich motifs in signaling proteins with their cognate domains. *FASEB J.* **2000**, *14*, 231−241.
(22) Burke, T. R.; Lee, K. Phosphotyrosyl mimetics in the development of signal transduction inhibitors. *Acc. Chem. Res.* **2003**, *36*, 426−433.
(23) Jeannotte, G.; Lubell, W. D. Large Structural Modification with Conserved Conformation: Analysis of Delta(3)-Fused Aryl Prolines in Model beta-Turns. *J. Am. Chem. Soc.* **2004**, *126*, 14334−14335.
(24) Grellier, P.; Vendeville, S.; Joyeau, R.; Bastos, I. M.; Drobecq, H. et al. Trypanosoma cruzi prolyl oligopeptidase Tc80 is involved in nonphagocytic mammalian cell invasion by trypomastigotes. *J. Biol. Chem.* **2001**, *276*, 47078−47086.
(25) Willand, N.; Joossens, J.; Gesquière, J.-C.; Tartar, A. L.; Evans, M. D. et al. Solid and solution phase synthesis of the 2-cyanopyrrolidide DPP-IV inhibitor NVP-DPP728. *Tetrahedron* **2002**, *58*, 5741−5746.
(26) Smet, C.; Sambo, A. V.; Wieruszeski, J. M.; Leroy, A.; Landrieu, I.; et al. The peptidyl prolyl cis/trans-isomerase Pin1 recognizes the phospho-Thr212-Pro213 site on Tau. *Biochemistry* **2004**, *43*, 2032−2040.
(27) Widmer, H.; Jahnke, W. Protein NMR in biomedical research. *Cell. Mol. Life Sci.* **2004**, *61*, 580−599.
(28) Hajduk, P. J.; Meadows, R. P.; Fesik, S. W. Discovering high-affinity ligands for proteins. *Science* **1997**, *278*, 497, 499.
(29) Hajduk, P. J.; Gerfin, T.; Boehlen, J. M.; Haberli, M.; Marek, D.; et al. High-throughput nuclear magnetic resonance-based screening. *J. Med. Chem.* **1999**, *42*, 2315−2317.
(30) Hamdane, M.; Smet, C.; Sambo, A. V.; Leroy, A.; Wieruszeski, J. M.; et al. Pin1: a therapeutic target in Alzheimer neurodegeneration. *J. Mol. Neurosci.* **2002**, *19*, 275−287.

JM0500119